Earth and Space Science

RESEARCH ARTICLE
10.1029/2018EA000415

Distribution of CO_2 in Western Pacific, Studied Using Isotope Data Made in Taiwan, OCO-2 Satellite Retrievals, and CarbonTracker Products

Amzad H. Laskar[1,2], Li-Ching Lin[1,3], Xun Jiang[4], and Mao-Chang Liang[1,3]

[1]Research Center for Environmental Changes, Academia Sinica, Taipei, Taiwan, [2]Now at Institute for Marine and Atmospheric Research Utrecht, Utrecht University, Utrecht, Netherlands, [3]Now at Institute of Earth Sciences, Academia Sinica, Taipei, Taiwan, [4]Department of Earth and Atmospheric Sciences, University of Houston, Houston, TX, USA

Key Points:
- We report more than three years mixing ratio of CO_2 and its stable isotope data in Taipei
- We studied the influence of long range transported CO_2 over Taiwan
- The elevated CO_2 in Taipei is mainly due to local anthropogenic emissions

Supporting Information:
- Supporting Information S1

Correspondence to:
M.-C. Liang,
mcl@gate.sinica.edu.tw

Citation:
Laskar, A. H., Lin, L.-C., Jiang, X., & Liang, M.-C. (2018). Distribution of CO_2 in western Pacific, studied using isotope data made in Taiwan, OCO-2 satellite retrievals, and CarbonTracker products. *Earth and Space Science*, *5*, 827–842. https://doi.org/10.1029/2018EA000415

Received 26 MAY 2018
Accepted 20 OCT 2018
Accepted article online 8 NOV 2018
Published online 29 NOV 2018

Abstract To assess sources and processes that affect the variability of CO_2 at local to regional scales, we have analyzed the mixing ratio [CO_2] and stable isotopic compositions ($\delta^{13}C$ and $\delta^{18}O$) of atmospheric CO_2 for three years (2014–2016) in urban and sub-urban areas in Taipei, Taiwan. The data are compared with those from some background sites, viz., Lulin, Mauna Loa, and Minamitorishima, to evaluate how local emissions affect CO_2 level regionally. [CO_2] over the urban and sub-urban stations are significantly higher than that observed at the three aforementioned remote sites mainly due to local emissions, which partly mask the seasonal cycle caused by photosynthesis and respiration. Likewise, significantly low $\delta^{13}C$ and $\delta^{18}O$ values observed at two Taipei stations also point to anthropogenic emissions. The seasonal cycles in [CO_2] and in the isotopic compositions are retrieved using the ensemble empirical mode decomposition method. Regional impact is assessed using CO_2 products from the Orbiting Carbon Observatory-2 satellite, the NOAA/EARL CarbonTracker project, and meteorological data from European Centre for Medium range Weather Forecast-Interim. We found that besides local emissions, Taiwan is largely affected by external CO_2 in winter and spring originated from north, west and southwest landmasses. In winter air masses with elevated CO_2 concentrations, originated in eastern China influence Taipei. In spring season, about 2 ppmv enhancement in CO_2 observed at the top of Lulin, a high mountain station (2.8 km), could be linked to CO_2 produced by biomass burning in the southeast Asian countries and transported to the region by easterly winds.

Plain Language Summary We presented CO_2 mixing ratio and stable isotope data, measured for more than three years in an urban and a sub-urban station in Taipei to identify their sources and asses the spatial heterogeneity and their influence on a regional scale. We also combined ground based observation by NOAA at a high mountain station in the central Taiwan with Orbital Carbon Observatory (OCO-2) satellite data, Carbon Tracker data and ECMWF wind data to identify the long-range transported CO_2 over the region in different seasons. We showed that Taiwan and its surrounding regions are affected by CO_2 from Eastern China in winter and south-east Asia in spring. The winter season pollutants are due to anthropogenic emissions in China and is transported by the strong winter monsoon. During the spring time, easterlies carry pollutants produced by massive biomass burning along with fossil fuel combustion in the south Asian countries.

1. Introduction

The level of CO_2 has been increasing in the Earth's atmosphere primarily due to fossil fuel burning and deforestation. This rise of CO_2 is a main driver of climate change, and hence considerable efforts have been made to characterize its spatial and temporal variations. Coupled measurements of mixing ratios and isotopic compositions for atmospheric CO_2 are widely carried out on sites far from anthropogenic sources (Ciais et al., 1995; Keeling et al., 1989, 1995; Mook et al., 1983; Tans et al., 1990; NOAA-ESRL global air sampling: http://www.esrl.noaa.gov/gmd/ccgg/). Urban emission is of particular interest, as this contributes about 75% of the global anthropogenic emissions (International Energy Agency, 2008; World Bank, 2010) and is projected to increase further in the coming decades (Duren & Miller, 2012). Therefore, studying CO_2, its sources, and spatial distribution in urban areas are important. Cities are primary targets for strategic emission reduction, and hence details of emissions from individual source sectors in urban areas are necessary for

policymakers to implement emission reduction strategies. In urban areas, contribution of the anthropogenic emission to the level of atmospheric CO_2 is generally estimated by combining fossil fuel consumption and its isotopic composition (Andres et al., 2000; Tans, 1981). Detailed studies in urban areas combining both isotope and mixing ratios, are relatively limited (e.g., Dallas, TX (Clark-Thorne & Yapp, 2003); Budapest, Hungary, and Krakow, Poland (Demeny & Haszpra, 2002; Kuc, 1986, 1991; Kuc et al., 2007; Kuc & Zimnoch, 1998); Salt Lake City, UT (Bush et al., 2007; Pataki, Bowling, & Ehleringer, 2003; Pataki et al., 2006, 2007), Paris, France (Widory & Javoy, 2003); Los Angeles, California (Newman et al., 2008); Melbourne (Coutts et al., 2007); Bangalore, India (Guha & Ghosh, 2014) and Taipei (Laskar et al., 2016a)). It is also important to understand how CO_2 concentrations in the atmosphere of urban source regions change with time. Recently the launches of CO_2 satellites such as GOSAT (Kuze et al., 2009; Yokota et al., 2009), OCO-2 (Miller et al., 2007; Worden et al., 2016; Wunch et al., 2016) and data-model integrated CarbonTracker project (Peters et al., 2007) offer new opportunities to monitor the distribution of anthropogenic emission globally. Attempts with applying remote sensing technique to probe CO_2 at local scales have been shown to be promising (e.g., see Kort et al., 2012). Nevertheless, ground-based studies in urban environments can complement at local scales.

Stable isotopic compositions ($\delta^{13}C$ and $\delta^{18}O$) in atmospheric CO_2 are useful tracers for identifying the sources and sinks of CO_2 (e.g., see Laskar et al., 2016a; Liang et al., 2018). Major sources of CO_2 are anthropogenic emissions from fossil fuel combustion, biomass burning, and plant and soil respiration; and major sinks are due to terrestrial and oceanic uptakes. CO_2 molecules from these sources impart $\delta^{13}C$ and $\delta^{18}O$ values to the atmosphere that can be used as tracers for constraining their sources and sinks at various temporal and spatial scales (Francey et al., 1985; Fung et al., 1997; Keeling et al., 1989; Laskar et al., 2016a). Isotopic compositions in the atmospheric CO_2 in urban and sub-urban areas can also provide important information for local processes such as biological emissions. So far, no isotopic study in atmospheric CO_2 has been conducted systematically in any part of Taiwan. Taipei, with a population of ~2.7 million (7.0 million in big metropolitan Taipei), is the largest city in Taiwan. Taiwan's net emission of CO_2 in 2015 was ~250,000 kiloton, out of which ~67% and ~17% were produced from energy and industrial manufacturing sectors, respectively ((http://unfccc.saveoursky.org.tw/2017nir/uploads/00_abstract_en.pdf). On per capita basis, Taiwan (10.9 tCO_2 per capita) is, in general, higher than most of the other Asian countries. A major part of this emission is contributed by big cities such as Taipei. In contrast, the total CO_2 emission from Asian countries is ~40% of the world total (International Energy Agency, 2017); China alone is 28%. Being in the down winds of China and southeast Asia countries, Taiwan is an ideal place for assessing regional anthropogenic impacts. A systematic source speciation is also important for the current deep decarbonization initiative of Taiwan.

The emphases of the available studies in the region are mainly focused on the influences of pollutants from the Asian land masses on the region (e.g., Ashfold et al., 2015; Chuang et al., 2016; Ou-Yang et al., 2015; Pochanart et al., 2004). The region near the sea level encounters prevailing wind from northeast in winter–spring (November–May) and from southwest during summer (June–September) (Chang et al., 2005; Laskar et al., 2014; Liu et al., 2001; Metzger, 2003; Rangarajan et al., 2017). It is well known that northwestern Pacific region is affected by the pollutants from Asian continent, especially in late winter to spring seasons when winter monsoon overwhelms the regional transport and mixing of air masses (Chao et al., 1996; Crutzen & Andreae, 1990; D'Asaro et al., 2014; Fu et al., 1983; Laskar et al., 2014; Qin et al., 2016; Thompson et al., 2001). Large Asian land masses, China in particular, in the north and northwest contribute massive atmospheric pollutants. Because of rapid urbanization in recent years in the east Asia, increased emissions of carbon, sulfur, and nitrogen bearing compounds have been reported to affect air quality in the northern Pacific region (Akimoto, 2003; Ohara et al., 2007; Wild & Akimoto, 2001). Air pollutants have also been found to transport from east Asia to the North America by easterly (Ambrose et al., 2011; Cooper et al., 2010; Jaffe et al., 2003; Liang et al., 2004). The same easterly also brings pollutants from pronounced biomass burning in the Indochina region of peninsular southeast Asia in spring, affecting the regional air quality significantly (Lin et al., 2014; Liu et al., 2003; Ou-Yang et al., 2012, 2014; Pochanart et al., 2003; Reid et al., 2013; Wai & Tanner, 2014).

To understand the role of Asian continental outflow of pollutants and their effects on air quality, a number of intensive field campaigns have been conducted over the western Pacific region (e.g., PEM-West B, Hoell et al., 1997; BIBLE, Kondo et al., 2002; TRACEP, Jacob et al., 2003; and EAREX, Nakajima et al., 2007). Recently, the Seven South-East Asian Studies (7-SEAS) program was launched to investigate the impact of biomass

burning on clouds, atmospheric radiation, hydrological cycle, and regional weather and climate in the Indochina region (Chi et al., 2016; Lin et al., 2013; Reid et al., 2013; Tsay et al., 2013). All these studies showed that the anthropogenic emissions from southeast Asia could influence the composition of tropospheric air over the north and northwestern Pacific regions. However, studies related to the influence of the biomass burning on the emission of greenhouse gases over the western pacific region are limited (Ou-Yang et al., 2015). By analyzing the levels of CO_2 isotopocules measured in Taipei, Taiwan, we investigate the effect of local emissions and long-range transport on atmospheric CO_2 on a regional scale in east Asia.

We present nearly three years of observational data at an urban station (National Taiwan University Campus, NTU henceforth) from November 2013 to December 2016 and at a sub-urban station (Academia Sinica campus, AS henceforth) from January 2013 to December 2016 of metropolitan Taipei on the mixing ratio and stable isotopic compositions of atmospheric CO_2. The aims are to identify the sources of urban CO_2 in Taipei, factors controlling its temporal and spatial variations, influence of CO_2 transported from distant sources such as China, and impact of local emissions on the regional scale. In addition, we make comparison with the regional CO_2 mixing ratios measured at a remote site viz., Lulin (LLN, a high mountain station at the central mountain ridge of Taiwan) and at two oceanic stations, viz., Mauna Loa (MLO) and Minamitorishima, located at central and western Pacific Ocean, respectively to assess the long range transported CO_2 over the region. The monitoring stations of LLN and MLO are maintained by National Oceanic and Atmospheric Administration (NOAA) and Minamitorishima by Japan Meterological Agency (JMA). LLN atmospheric background observatory is situated at an altitude of ~2.8 km which is above the boundary mixed layer and hence record the regional background isotopic values. The effect of emission from the local cities such as Taipei to LLN is not significant. As shown earlier (Ou-Yang et al., 2014), it mainly receives air mass from southeast Asia in spring, Pacific in summer, and northern continents in winter. To assess the long-range transport of CO_2 in Taiwan, we also analyze data from Orbiting Carbon Observatory satellite-2 (OCO-2) and NOAA/Earth System Research Laboratory (ESRL) CarbonTracker (http://carbontracker.noaa.gov) project. Furthermore, the interpretation is complemented by analysis from European Center for Medium Range Weather Forcast (ECMWF)-Interim meteorological data, to fill in gap that OCO-2 and CarbonTracker cannot offer clear event studies at temporal resolutions for the present work e.g., biomass burning in Indochina countries in spring time.

2. Materials and Methods

2.1. Air Sampling

Air samples were collected from two stations: AS and NTU (Figure 1). AS is a sub-urban station, and the samples were collected from an open roof (~30 m above ground) of Institute of Earth Sciences Building (25°2′27″ N, 121°36′51″E). Urban air samples were collected over a grassland in front of the Department of Atmospheric Sciences, NTU (25°0′52″N, 121°32′20″E). The samples were collected at a point which was ~150 m away from the nearest traffic road. Samples were normally collected during day time, usually three samples a day at local times ~10:00, ~13:00, and ~16:00 hrs. Air samples were collected in ~1.5 L pyrex flasks and compressed to 2 bar in pressure using a membrane pump. The flasks, equipped with two high vacuum stopcocks, were first flushed with the ambient air for ~10 mins before sample collection. After flushing the downstream end stopcock was closed and allowed the pressure to build up to ~2 bar and then isolated by closing the other stopcock. The air pumping during flushing and sampling was carried out through a column packed with magnesium perchlorate to remove moisture. The perchlorate column reduced the moisture content from the ambient value of 70–90% to less than 1% relative humidity, checked using a LI-COR infrared gas analyzer (model 840A, LI-COR, USA). See, for example, Liang and Mahata (2015) for more details on air sampling.

2.2. CO_2 Extraction and Analyses

CO_2 was extracted from air mixture by cryogenic technique using a glass-made vacuum line, connected to a turbo pump. The vacuum line as well as the sample flask connection assembly including its head space was pumped to a high vacuum ($<10^{-3}$ torr) before starting the CO_2 extraction. Air in the flask was pumped through a series of five multi-coiled traps, with the first two immersed in dry ice-acetone slush (−77 °C) for trace moisture removal followed by three in liquid nitrogen (−196 °C). CO_2 was collected from the traps immersed in liquid nitrogen by repeated freeze–thaw technique at liquid nitrogen and dry ice temperatures for further removal of traces of water (e.g., see Laskar & Liang, 2016 for details). The air was pumped for

Figure 1. Map of Taiwan (left) along with sampling stations (AS and NTIU) in Taipei city (right). The location of Lulin observatory and coastal weather station at Keelung are shown in the left panel.

~30 minutes at a controlled rate of ~90 mL/min regulated by a mass flow controller. No significant isotopic fractionation caused by mass flow controller at this flow rate was observed, checked using several aliquots of CO_2 extracted from a high volume compressed air cylinder (~40 L at 2000 psi) (see Liang et al., 2016 for details).

The CO_2 samples were measured using a stable isotope ratio mass spectrometer (Thermo-Fisher MAT 253) in dual-inlet mode at Institute of Earth Sciences, Academia Sinica, Taiwan. CO_2 samples were measured against working standards WES, AS-2, and OZTECH. At the initial phase the working gas used was WES and AS-2. WES was prepared from mollusk shell carbonates by acid digestion and equilibrated with water at 25 °C to have isotopic ratios close to atmospheric CO_2 ($\delta^{13}C = -6.66$ ‰ with respect to VPDB and $\delta^{18}O = 40.14$ ‰ with respect to VSMOW; Mahata et al., 2012). AS-2 is a high purity commercial CO_2 with $\delta^{13}C = -32.54$ ‰ (VPDB) and $\delta^{18}O = 36.61$ ‰ (VSMOW) procured from a local supplier (Air Products and Chemicals, Inc.). From December, 2014 onward, the working gas used was OZTECH ($\delta^{13}C = -3.59$ ‰ and $\delta^{18}O = 24.96$ ‰) (Oztech Trading Corporation, USA). No detectable difference in isotopic compositions was observed between the analyses from the different working references (for details see Laskar & Liang, 2016; Laskar et al., 2016a, 2016b). All the $\delta^{13}C$ values presented in this work are expressed in VPDB scale and $\delta^{18}O$ in VSMOW scale. The reproducibility for air CO_2 measurements was established from aliquots of CO_2 extracted from the compressed air cylinder with CO_2 mixing ratio of ~388 ppmv. The 1-σ standard deviations for $\delta^{13}C$ and $\delta^{18}O$ were 0.07 and 0.08 ‰, respectively (Liang et al., 2016). We applied corrections for the interference of N_2O to CO_2 of +0.19 ‰ for the $\delta^{13}C$ values and + 0.27 ‰ for the $\delta^{18}O$ values (Sirignano et al., 2004). We also checked the validity of these corrections by passing CO_2 samples through a GC column and separating N_2O from CO_2 and measuring $\delta^{13}C$ and $\delta^{18}O$ values in the purified CO_2 (Laskar et al., 2016a; Laskar & Liang, 2016).

2.3. Measurements of CO_2 Mixing Ratio

For measurements of the mixing ratio of a CO_2 sample, a pyrex flask of volume ~350 cc was used. The flask was connected in series with the flask used for isotopic measurements. Flushing and sampling for both the flasks were done simultaneously. Mixing ratios were measured using a LI-COR infrared gas analyzer (model 840A, LI-COR, USA) at 4 Hz, smoothed with 20-s moving average. Air at ~2 bar pressure from the 350 cc flask was allowed to pass through the LI-COR at a flow rate of ~30 mL/min. When the concentration signal becomes stable (takes ~2 minutes), the value is recorded. For routine flask analysis, the analyzer was first calibrated against a working standard (compressed air in a cylinder) with a nominal value of CO_2 mixing ratio of 387.7 ppmv and a CO_2 free N_2 gas. The reproducibility of LI-COR was better than 1 ppmv. The working standard was calibrated using a commercial Picarro analyzer (model G1301, Picarro, USA) by a series of NOAA standards with CO_2 mixing ratios of 369.9, 392.0, 409.2, and 516.3 ppmv, with a precision (1-σ standard deviation) of 0.2 ppmv.

2.4. Seasonal Variation Analyzed Using Ensemble Empirical Mode Decomposition (EEMD)

A new sophisticated statistical data analysis scheme, *viz*. Ensemble Empirical Mode Decomposition (EEMD) is applied to delineate the seasonal cycles in mixing ratios as well as isotopic compositions (Wu & Huang, 2009) which otherwise may be obscured in the raw data. EEMD, an advanced version of the Empirical Mode Decomposition (EMD) that removes high-frequency components such as random noise (Chen & Ma, 2014), is a time–space analysis method in which white noise is added to provide a uniform reference frame in the time–frequency space. The added white noise is averaged out iteratively and the only persistent part that survives the averaging process is the component of the signal (original data), which is then treated as the true signal. This approach utilizes the advantage of the statistical characteristics of white noise that perturbs the signals and cancel itself out after serving its purpose. This is purely a noise-assisted data analysis method. For more details, see Chen and Ma (2014).

2.5. Orbiting Carbon Observatory-2 (OCO-2) Satellite Retrieved CO_2, CarbonTarcker CO_2, and ECMWF Wind Data

On a regional scale, satellite data in concert with ground-based measurements can be highly effective in investigating the seasonal and spatial characteristics of air pollutants, including location and magnitude of sources and sinks. Here, we compared OCO-2 satellite retrieved CO_2 with that observed at the ground level, along with a regional/global view from CarbonTracker and ECMWF-interim analysis.

The OCO-2 satellite, launched in July 2014, provides CO_2 with precision, resolution, and coverage needed to characterize CO_2 sources and sinks on regional and global scales (Crisp et al., 2004; Miller et al., 2007). It employs high-resolution spectra of reflected sunlight taken simultaneously in near-infrared (NIR) CO_2 (1.61-μm and 2.06-μm) and O_2 (0.765-μm) bands to retrieve the column-averaged CO_2 dry air volume-mixing ratio XCO_2 from space (Crisp et al., 2004, 2016; Kuang et al., 2002). Precision for the OCO-2 column CO_2 measurements is better than 1.5 ppm (Miller et al., 2007; Worden et al., 2016; Wunch et al., 2016). The OCO-2 column CO_2 (product version 7) are available at http://disc.sci.gsfc.nasa.gov/uui/datasets?keywords=OCO%20ACOS. Here, we used daily averaged (and then seasonally) CO_2 mixing ratios from September, 2014 to December, 2016 for identification of regional sources and transport of CO_2 with a grid size of $2° \times 2.5°$ in east Asia.

To check the spatial distribution and transport of pollutants at high resolution, we also analyzed CarbonTracker CO_2 data (Peters et al., 2007). CarbonTracker is a data assimilation system built by NOAA/ESRL to estimate the surface CO_2 exchange. It is used to analyze (reanalyze) the recent flux history of CO_2 using a state-of-the-art atmospheric transport model coupled to an ensemble Kalman filter. In addition, we presented wind speed and direction analysis from ECMWF-Interim analysis data (Dee et al., 2011) to assess the air mass trajectories, to infer transport of pollutants including CO_2 in the western Pacific region.

3. Results and Discussion

3.1. CO_2 Mixing Ratio

The atmospheric CO_2 mixing ratios over the urban and sub-urban stations are shown in Figure 2. In the urban station at NTU, the mixing ratio varies between 394 and 478 ppmv with an average of 420 ± 17 ppmv; at the sub-urban AS station, it varies between 391 and 449 ppmv with an average of 413 ± 11 ppmv. Most of the values are higher than that at MLO. Higher values of CO_2 mixing ratios at AS and NTU are mainly due to the contribution of CO_2 from local vehicle emission. The mixing ratios measured near Roosevelt Road, a busy traffic street in Taipei on 24th July, 2014 varies between 464 to 564 ppmv with an average of 515 ± 36 ppmv (Laskar et al., 2016a). The high values of the mixing ratios at NTU station, which is ~150 meters away from the Roosevelt road, is due to influence of vehicle exhaust. Similarly, the elevated CO_2 mixing ratio at AS station is due to vehicle emission from traffics nearby, in addition to local respiration (Laskar & Liang, 2016).

Seasonality or trend is not obviously seen from the raw mixing ratio data during the studied period (Table 1), unlike MLO where a clear seasonal cycle and trend are apparent (Figure 2). With EEMD analysis (Wu & Huang, 2009), seasonal variations are successfully retrieved, at amplitudes, in general, greater than that at MLO (Figures 2, 3). The reason for the obscured seasonal variations in the raw data is because of large temporal variation, in particular, the diurnal cycle of photosynthesis, respiration, anthropogenic emission, and sampling inhomogeneity in time. In urban areas, it was noted that seasonality in CO_2 mixing ratio is more

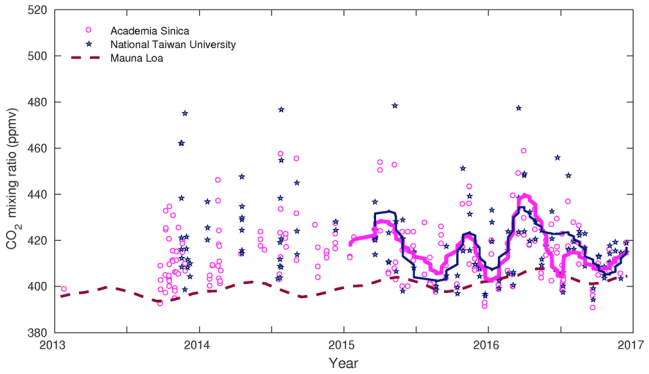

Figure 2. Time series of near surface atmospheric CO_2 mixing ratios at sub-urban station Academia Sinica (AS) campus and urban station National Taiwan University (NTU) campus. Monthly mixing ratios observed at Mauna Loa observatory during the same period are also shown for comparison. EEMD analysis for the Taipei data are shown by the blue and pink curves to show seasonality. We note that EEMD analysis could not be performed robustly before 2015 due to insufficient data.

prominent in night time (Pataki, Bowling, & Ehleringer, 2003), due to reduced photosynthetic uptake. All the measurements reported in this work were made in day time, which is another reason for absence of a pronounced seasonality in the raw data. Vegetation in Taiwan is mostly evergreen and hence difference in photosynthetic activity between winter and summer is small, unlike other cities such as Salt Lake City, USA (Pataki, Bowling, & Ehleringer, 2003). In addition, Taiwan is a relatively small island (the sampling spots are less than 40 km from oceans) and insurgence of marine air especially in winter from north and summer from south-east is typical (Rangarajan et al., 2017). A combined effect of the above mentioned factors is responsible for the less clear seasonality in the CO_2 mixing ratio in Taipei. We believe the EEMD retrieved variations are real because of the strong correlation between $\delta^{13}C$ and concentration of CO_2 observed for a binary mixing of two components (discussed later). Similar to that found earlier (e.g., see Jiang et al., 2012), semi-annual variations are significant, with amplitudes comparable to the annual cycles.

Figure 3 shows a comparison between the mixing ratios at the three remote stations and the OCO-2 satellite retrievals with the present data after EEMD analysis. The remote stations are the MLO observatory located around the middle of Pacific, Minamitorishima at the western part of Pacific, and LLN, a high mountain station in the central part of Taiwan. Though the seasonal variations at the studied stations are in phase with that observed in remote stations, the large amplitude and overall higher mixing ratios are apparent, due to local emissions. A difference of 2 to 3 ppmv in the mixing ratio between the OCO-2 satellite retrievals and ground measurements is observed over the region. This is because the CO_2 level at the surface is in general larger than the column averaged CO_2 from OCO-2 (see, for example, Jiang et al., 2016 for a composition of surface CO_2 with GOSAT XCO_2, which has a similar averaging kernel as OCO-2). One interesting observation is that during the late winter to the spring, the mixing ratio at LLN is higher by ~2 ppmv than that at the other Pacific Ocean stations. Also the excess of CO_2 in winter–spring at LLN has increased significantly from 2013 to 2016. This extra CO_2 observed at LLN could be either local, regional, or a combination of both, and we examine the source(s) below.

To identify the source(s) of the extra CO_2 at LLN in late winter to spring, we first analyzed the satellite data over the region. Figure 4 shows the OCO-2 column CO_2 averaged over summer (July 2015 – Sep 2015), winter (Nov 2015 – Jan 2016) and spring (Mar 2016 – May 2016) seasons. There is no identifiable hot spot over Taiwan, indicating that the local emission in Taiwan including urban and industrial areas is probably not significant in affecting the level of CO_2 on a regional scale. The OCO-2 summer data does not show much change in CO_2 concentration over Taiwan and its surrounding regions, but during the winter and spring seasons, a significant gradient from the east and southeast Asia towards Taiwan is clearly seen (Figure 4). This indicates that a source of the excessive CO_2 at LLN in late winter and spring seasons is likely to be long-range

Table 1
Summary of the Seasonal Mixing Ratios and Stable Isotopic Compositions at Academia Sinica and National Taiwan University Campus from 2013 to 2016. May-Oct and Nov-April are Considered as Summer and Winter Respectively

	Academia Sinica			National Taiwan University		
Season	CO_2 Conc. (ppmv)	$\delta^{13}C$ (‰) (VPDB)	$\delta^{18}O$ (‰) (VSMOW)	CO_2 Conc. (ppmv)	$\delta^{13}C$ (‰) (VPDB)	$\delta^{18}O$ (‰) (VSMOW)
Summer 2013	408.5 ± 12.2	−8.88 ± 0.67	40.46 ± 0.52	NA	NA	NA
Winter 2013–2014	412.5 ± 10.4	−8.92 ± 0.50	40.81 ± 0.53	425.7 ± 19.2	−9.39 ± 0.55	40.48 ± 0.71
Summer 2014	420.1 ± 14.4	−9.41 ± 0.77	40.48 ± 0.78	425.2 ± 22.2	−9.39 ± 0.87	40.14 ± 1.25
Winter 2014–2015	417.5 ± 6.2	−9.21 ± 0.50	41.11 ± 0.55	423.2 ± 15.5	−9.55 ± 0.67	41.23 ± 0.57
Summer 2015	411.6 ± 10.7	−9.23 ± 0.57	40.81 ± 0.65	415.7 ± 13.7	−9.18 ± 0.49	40.72 ± 0.49
Winter 2015–2016	415.5 ± 14.1	−9.45 ± 0.55	40.96 ± 0.48	419.4 ± 16.9	−9.52 ± 0.65	40.89 ± 0.80
Summer 2016	410.5 ± 10.6	−9.14 ± 0.48	41.18 ± 0.49	416.4 ± 14.9	−9.30 ± 0.75	40.75 ± 0.59
Winter 2016	412.8 ± 4.9	−8.89 ± 0.23	41.34 ± 1.12	414.8 ± 4.7	−9.08 ± 0.23	40.74 ± 0.15

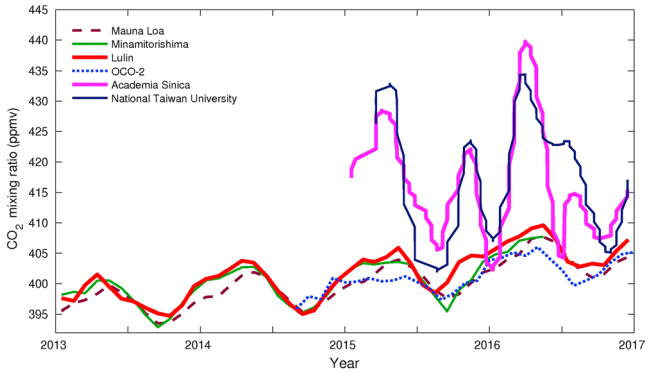

Figure 3. Monthly averaged atmospheric CO_2 mixing ratios at Mauna Loa (mid-Pacific), Minamitorishima (western Pacific) and Lulin observatory (Taiwan). EEMD analysis of the ground level mixing ratios at the two studied stations are overplotted. Atmospheric column CO_2 mixing ratio retrieved from the orbital carbon Observatory-2 (OCO-2) satellite sampled over Taiwan is also shown.

transported from east and southeast Asian countries. Five-day backward trajectories from the Hybrid Single Particle Lagrangian Integrated Trajectory (HYSPLIT) model (Draxler & Rolph, 2014) for air masses reaching Taipei and LLN in summer, spring, and winter are also plotted over the OCO-2 images (Figure 4). In the summer, the air masses reaching Taipei and LLN originate from the Pacific Ocean and from northern continents during winter. In spring, the high mountain site (LLN) is affected by long-range transported air masses from southeast Asian countries, while Taipei remains influenced by high latitude air masses (mainly from north). The cold fronts developed in the Siberian high pressure system in winter move southeastward, driving China pollution outflow into the western Pacific region (Liu et al., 2003; Wang et al., 2003; Zhang et al., 1997). The spring (March–May) corresponds to the transition from winter to summer monsoon and during which convection becomes significant. The convection enhances atmospheric mixing vertically and lifts up pollutants from the ground level in southwestern China. A part of pollutants can be picked up by the easterlies (Bey et al., 2001; Nieuwolt, 1977). During this time period, southeast Asia is rather warm and dry, a condition favorable for biomass burning (mainly agricultural wastes; Nguyen et al., 1994; Vadrevu et al., 2012; Lin et al., 2014). Lulin, located at the downwind site observes the plumes.

To aid in detail the lateral movement of CO_2, CarbonTracker CO_2 and ECMWF wind vector fields for winter of 2015 (Figure 5a) and spring of 2016 (Figure 5b) are shown. In winter, it is clearly observed that during the selected six days (23–28 November, 2015), air masses with high CO_2 concentration, emitted mainly in the eastern China, moved south-eastward, influencing Taiwan significantly, with the column CO_2 (weighted

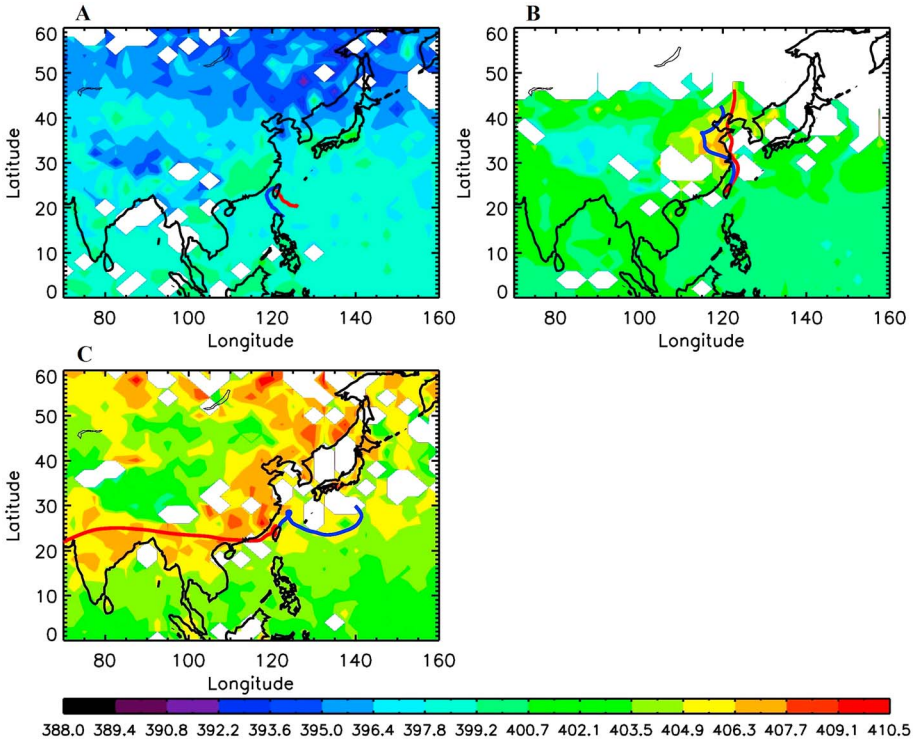

Figure 4. Column CO_2 from OCO-2 satellite smoothed at a spatial resolution of 2° × 2.5° over Taiwan and its surroundings in (a) summer (Jun 2015-Aug 2015), (B) winter (Nov 2015-Jan 2016) and (C) spring (Mar 2016-May 2016). The values are reported in ppmv. To show the regional influence, the HYSPLIT 120 hours back trajectory plots (using GDAS meteorological data, Draxler & Rolph, 2014) ending at Lulin (red curve) and Taipei (blue curve) for a day each of summer, winter, and spring are shown; the selected days are august 1, 2015, December 15, 2015, and May 1, 2016.

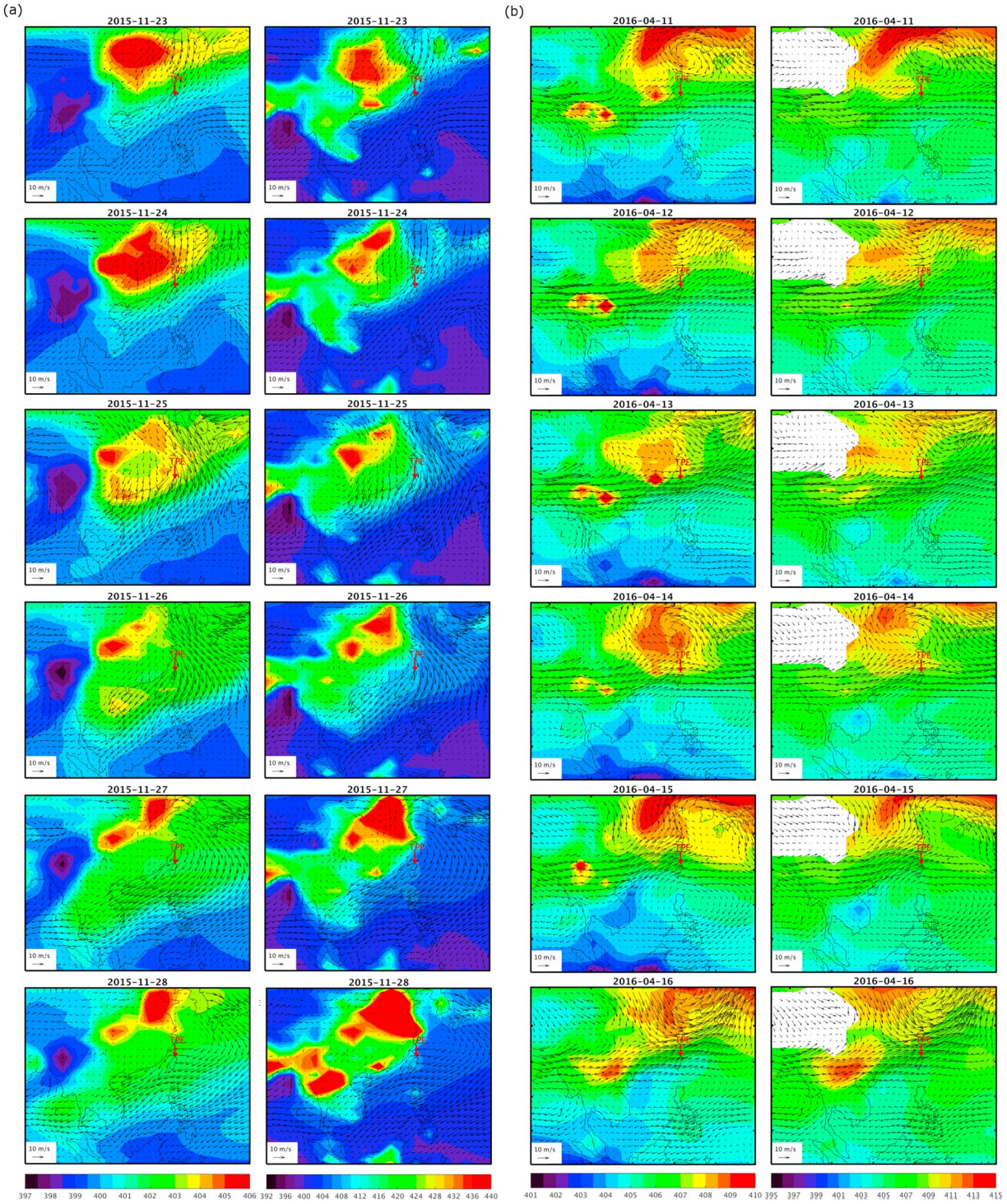

Figure 5. CarbonTracker CO_2 (color coded) and ECMWF-interim analysis wind (arrows) for the selected events in the winter of 2015 (a) and spring of 2016 (b) The left panels (vertical panels 1 and 3) of each one are the column CO_2 obtained by weighting the model CO_2 with the OCO-2 weighting function. The right panels (vertical panels 2 and 4) are the CO_2 volume mixing ratio at the surface (a) and 750 mbar (b). the wind fields in (a) and (b) are for the surface and 750 mbar, respectively.

with OCO-2 weighting function; left panels of Figure 5a) changing from ~400 ppmv on the 23rd to ~404 ppmv on the 25th. The inference of China origin of air masses is supported by the ECMWF-Interim surface wind at 10 m height shown by the arrows; the surface CO_2 concentrations are shown in the right panels (vertical panels 2 and 3 in Figure 5). In springtime (11–16 April, 2016), the wind at 750 mbar blew north-

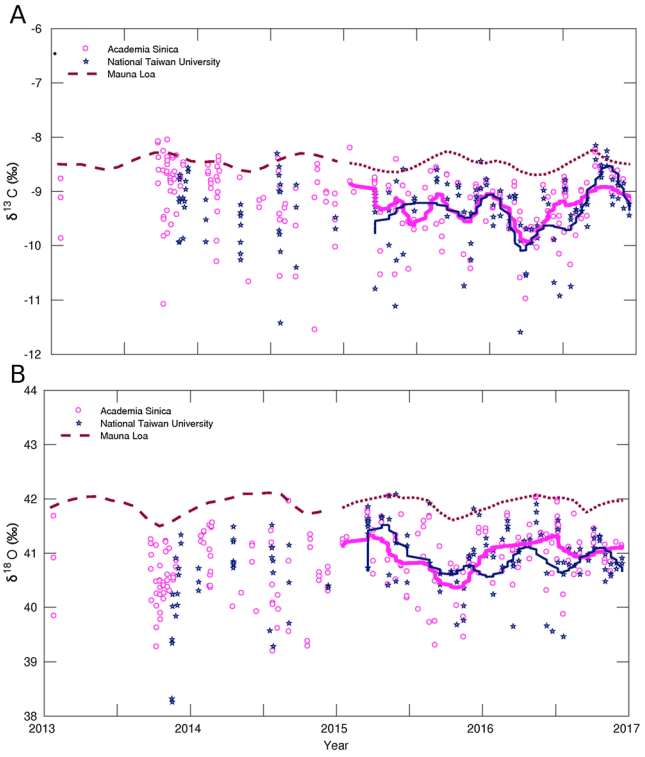

Figure 6. Time series of stable carbon and oxygen isotopic compositions ($\delta^{13}C$ and $\delta^{18}O$) at AS and NTU. For comparison, those observed at Mauna Loa are also shown. EEMD analysis of the data (dark blue and pink line) show seasonality which is in phase with that observed at Mauna Loa. EEMD analysis could not be performed before 2015 due to insufficient data.

eastwards, transporting pollutants from south Asia. The CO_2 concentrations at 750 mbar, the pressure altitude of LLN, are shown in the right panels of Figure 5b. High level of CO_2 was also reported by OCO-2 (Figure 4C). During this period, a noticeable biomass burning in the region was noted (see the left panels of Figure 4C for the column CO_2 level). 2016 being an El Nino year, the region experienced relatively hot and dry weather (Thirumalai et al., 2017) enhancing biomass burning and forest fires which caused elevated CO_2 level at LLN.

There is no obvious difference in summertime CO_2 mixing ratio between LLN and other two remote Pacific Ocean stations, indicating absence of noticeable pollutants reaching LLN. This is mainly due to predominance of clean air masses from South China Sea and Pacific Ocean (Laskar et al., 2014; Rangarajan et al., 2017), preventing transport of air pollutants from the northern continents and southeast Asian countries to the region.

3.2. Stable Isotope Composition in Urban and Sub-Urban CO_2

Time series of the stable isotope compositions ($\delta^{13}C$ and $\delta^{18}O$) in the two stations are shown in Figure 6. In the urban station, $\delta^{13}C$ values vary between −8.15 and − 11.60 ‰ with an average of −9.35 ± 0.63 ‰; and in the sub-urban station it varies between −8.00 and − 10.60 ‰ with an average of −9.08 ± 0.49 ‰. The values are in general lower than that observed at MLO, indicating additional contribution from local and/or regional anthropogenic emission.

The local fossil fuel combusted CO_2 has a $\delta^{13}C$ value of −27.2 ‰ (Figure 7). Keeling graphical analysis, representing a simple mixing of two gases, relates the isotopic composition ($\delta^{13}C$, $\delta^{18}O$, etc.) and the inverse of the concentration of the mixture (Keeling et al., 1979; Pataki, Bowling, & Ehleringer, 2003; Pataki, Ehleringer, et al., 2003) gives an intercept of −27.2 ‰, the anthropogenic end-member. The isotope data used for the Keeling plot in Figure 7 are obtained from direct car exhaust, air CO_2 over a urban traffic street (Roosevelt road, Taipei), regional background CO_2 collected over the ocean (Laskar & Liang, 2016) and high concentration air CO_2 collected inside the Hsuehshan tunnel, a ~13 km long highway in Taiwan (Laskar et al., 2016a). The respired CO_2 by C_3 type plants has similar values as the derived anthropogenic end-member (Laskar et al., 2013, 2016c). Similar to CO_2 mixing ratio, no systematic trend or clear seasonal variation are observed in $\delta^{13}C$ (Table 1), for the same

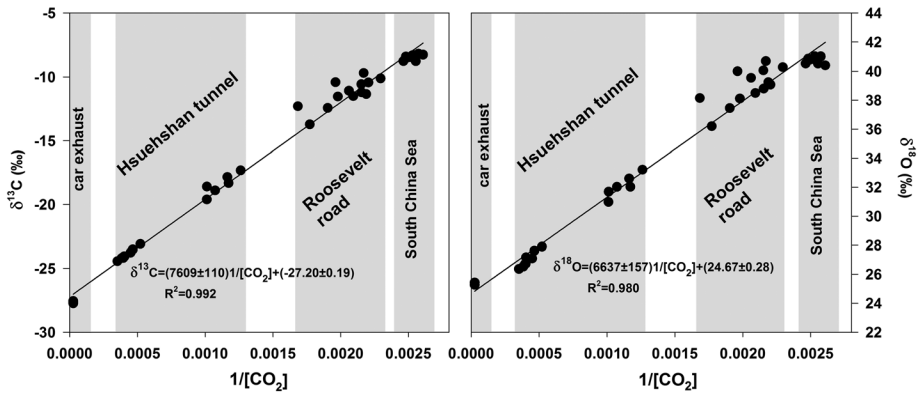

Figure 7. Keeling plots for $\delta^{13}C$ and $\delta^{18}O$, plotted in different environments with different extent of anthropogenic emission including direct exhaust. The extreme values are those observed over the ocean (background) and car exhausts (anthropogenic). The intermediate isotopic data are obtained from air CO_2 collected near a traffic street (Roosevelt road, Taipei) and a tunnel highway (Hsuehshan, Taiwan) (data sources: Laskar & Liang, 2016; Laksar et al., 2016a).

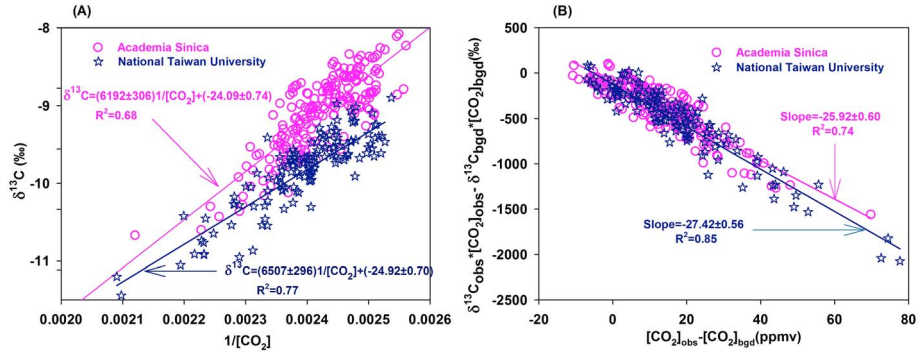

Figure 8. (a) Keeling and (b) Miller-Tans plots for $\delta^{13}C$ in atmospheric CO_2 over the campuses of Academia Sinica and National Taiwan University.

reason as $[CO_2]$ that sampling inhomogeneity is a main cause, in particular the absence of night time samples. However, the EEMD analysis presented in Figure 6 shows the retrieved seasonality (annual and semi-annual combined). We see that the variation in $\delta^{13}C$ is out of phase with the $[CO_2]$ (Figure 3), verifying the robustness of the EEMD in retrieving the seasonal cycles.

The $\delta^{18}O$ values vary in the range of 38.32 to 42.09 ‰ (mean 40.81 ± 0.64 ‰) and 39.30 to 44.29 ‰ (mean 40.90 ± 0.61 ‰) at NTU and AS, respectively. The EEMD retrieved seasonal cycle in shown in Figure 6. Most of the $\delta^{18}O$ values, like $\delta^{13}C$ are also lower than that observed at MLO. These lower values are due to contribution of CO_2 from combustion. The major source of oxygen in CO_2 emitted from fossil fuel burning is the atmospheric O_2 with $\delta^{18}O$ value of ~23.5 ‰ (Luz & Barkan, 2011; Jurikova et al., 2016), which is much less than the $\delta^{18}O$ value of atmospheric CO_2 (~40 ‰). Similar to $\delta^{13}C$, Keeling analysis is applied to identify the $\delta^{18}O$ end member (Figure 7). The deviation or scattering of the data points in Figure 7 for both $\delta^{13}C$ and $\delta^{18}O$, especially in the case of the traffic street Roosevelt road, is partly due to contribution from other sources of CO_2 such as respiration. In other cases such as tunnel CO_2, car exhausts and samples over the ocean, the contribution from any third component is expected to be low or absent. The intercept 24.6 ‰ in Figure 7 is slightly higher than that of atmospheric O_2 (~23.5 ‰). This difference is probably due to contribution from other sources such as respiration and exchange of oxygen isotopes of CO_2 with leaf and soil waters. More variation in $\delta^{18}O$ compared to $\delta^{13}C$ is again due to the fact that the oxygen isotopes in CO_2 can exchange with the oxygen isotopes in liquid phase of water when they come in contact (Gemery et al., 1996), and the process is sensitive to temperature (Benninkmeijer et al., 1983). As discussed in the case of $[CO_2]$, an additional small peak around the end of 2015 is observed in the isotopic time series data, particularly in $\delta^{13}C$ (Figure 6), the semi-annual variation as discussed by Jiang et al. (2012).

To identify the isotopic composition of regional anthropogenic sources that affect local CO_2, Keeling and Miller-Tans graphical approaches are used and compared. Keeling analysis is useful specifically when the background concentration and its isotopic composition are constant. Figure 8A shows the Keeling plots for $\delta^{13}C$ at AS and NTU. However, from nearby rather clean stations, for example, Dongsha Island (Ou-Yang et al., 2015), the level of CO_2 mixing ratio varies seasonally and differs from that of MLO, indicating regional CO_2 emission and natural cycling. In such a case, Miller-Tans' approach (Miller & Tans, 2003) is more appropriate for quantifying sources and processes that affect CO_2 isotopocules at a local scale. The Miller-Tans equation for source identification can be formulated as:

$$\delta^{13}C_{obs}[CO_2]_{obs} - \delta^{13}C_{bgd}[CO_2]_{bgd} = \delta^{13}C_{src}\left([CO_2]_{obs} - [CO_2]_{bgd}\right),$$

where $[CO_2]$ is the CO_2 mixing ratio and the subscripts 'obs,' 'bgd,' and 'src' represent the values of the parameters associated with observed, background and source, respectively. In absence of any systematic background values of $[CO_2]$ and $\delta^{13}C$ in the studied region, we assume that the background $\delta^{13}C$ and $[CO_2]$ are similar to the monthly average values observed at MLO during the sampling periods.

Table 2
Season-Wise Fraction of Anthropogenic CO_2 in Percentage at Urban and Sub-Urban Stations Estimated Using Observed $\delta^{13}C$ Values and Assuming Monthly Mean $\delta^{13}C$ Values Observed at Mauna Loa as the Background. A Year is Divided Into Summer (May to October) and Winter (November to the Following Year April)

	Fraction of anthropogenic CO_2 in %	
Season	Urban station (NTU)	Sub-urban station (AS)
Summer 2013	NA	2.0 ± 3.5
Winter 2013–2014	4.7 ± 2.9	2.2 ± 2.7
Summer 2014	4.7 ± 4.6	4.8 ± 4.1
Winter 2014–2015	5.5 ± 3.5	3.7 ± 2.7
Summer 2015	3.6 ± 2.6	3.8 ± 3.0
Winter 2015–2016	5.3 ± 3.4	5.0 ± 2.9
Summer 2016	4.3 ± 4.0	3.4 ± 2.6
Winter 2016	3.0 ± 1.3	2.0 ± 1.3

Figure 8B shows the Miller-Tans plots at AS and NTU. The slope of the Miller-Tans plot gives the $\delta^{13}C$ value of the source(s). The slopes are slightly different for the two stations, indicating variation in the sources at the two stations. In both the stations, the main source of CO_2 is local anthropogenic emission, and $\delta^{13}C$ value of which is −27.2 ‰ (Laskar & Liang, 2016; see also Figure 7). In the present case, the slopes are −27.4 ± 0.6 ‰ and − 25.9 ± 0.6 ‰, which are close to the vehicle exhaust $\delta^{13}C$ value (−27.2 ‰), particularly for the urban station. The relatively lower slope at AS is probably due to more contribution from biospheric respiration at this station. Respiration could produce CO_2 with a wide range of $\delta^{13}C$ values, because of large intra- and inter-inhomogeneity between species. For example, soil and plant respired CO_2 fall in the range of −19 to −32 ‰ with an average of −27 ‰ for C_3 type of vegetation, and the values are −9 to −19 ‰ with an average of −13 ‰ for C_4 type (Deines, 1980; Laskar et al., 2013, 2016c; Mehta et al., 2013). It is to be noted that the $\delta^{13}C$ values of CO_2 originated from C_3 type plant respiration is indistinguishable from that emitted by fossil fuel combustion. The sampling spot at NTU is a grassland of dimension ~ 50 m × 50 m, surrounded by thick C_3 plants, and AS also has grasslands. The tropical warm grasses are mainly C_4 type. A few grass samples near the NTU sampling spot were measured for $\delta^{13}C$ and found values in the range of −15 to −17 ‰ with an average value of −16 ‰ (Laskar & Liang, 2016). However, the signature of the C_4 vegetation is not significant especially at the urban station (NTU). The slightly higher slope at AS could be due to some contribution from C_4 plant respiration. The influence from respiration especially from C_4 plants may vary from place to place and is probably relatively higher at the sub-urban station. In the present case, Miller-Tans approach, with seasonally varying background data observed at Mauna Loa, better constrains the sources compared to the Keeling approach (see Figure 8). The result indicates that the background CO_2 in the studied locations is set regionally. The local emission largely affects the variations of the local CO_2 isotopocules and their contribution over a regional scale is not significant as discussed earlier. A more detail comparison also shows that the background levels also affect the source identification (see below), which demands the need of a systematic regional background monitoring for proper assessment.

3.3. Estimation of Anthropogenic CO_2 Fraction Using $\delta^{13}C$

From the Keeling and Miller-Tans analyses presented above, it is obvious that a significant fraction of anthropogenic CO_2 produced locally is present in the atmospheric CO_2 at the urban and sub-urban sites. We estimate the anthropogenic fraction of CO_2 based on a two-component mixing model given as $\delta^{13}C_{obs} = f_{anth} \times \delta_{anth} + (1\text{-}f_{anth}) \times \delta^{13}C_{bgd}$, where $\delta^{13}C_{obs}$ and $\delta^{13}C_{bgd}$ are the $\delta^{13}C$ values in air CO_2 observed at a given time and background CO_2, respectively (Laskar et al., 2016a). The regional background values are assumed to be the values observed at MLO. The 'anthropogenic' end member for $\delta^{13}C$ (−27.2 ‰) is taken from Figure 7. Table 2 shows the season-wise local anthropogenic CO_2 contributions from 2013 to 2016. Anthropogenic CO_2 fraction varies between 3.0 to 5.5% at NTU and 2.0 to 5.0% at AS, and no trend and systematic difference between winter and summer seasons are observed. While estimating average seasonal anthropogenic contribution using $\delta^{13}C$ values, we did not consider the contribution from other sources such as respiration. As the dominant vegetation in the region is C_3 type with an average $\delta^{13}C$ value which is similar to the anthropogenic CO_2, it is not possible to partition the contribution from these two sources using $\delta^{13}C$ alone (Laskar et al., 2016a; Laskar & Liang, 2016). However, we note that these estimations agree with some pervious ones utilizing CO_2 clumped isotopes (Laskar et al., 2016a). We believe the same holds for NTU site for two reasons. First, the site is located

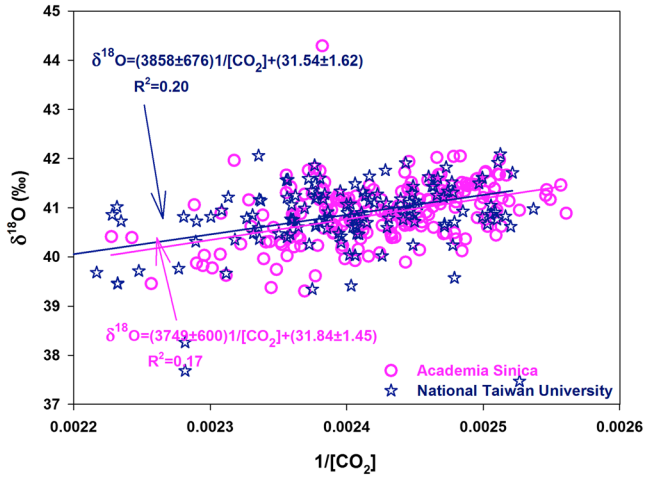

Figure 9. Oxygen isotope keeling plot for atmospheric CO_2 over the campuses of Academia Sinica and National Taiwan University.

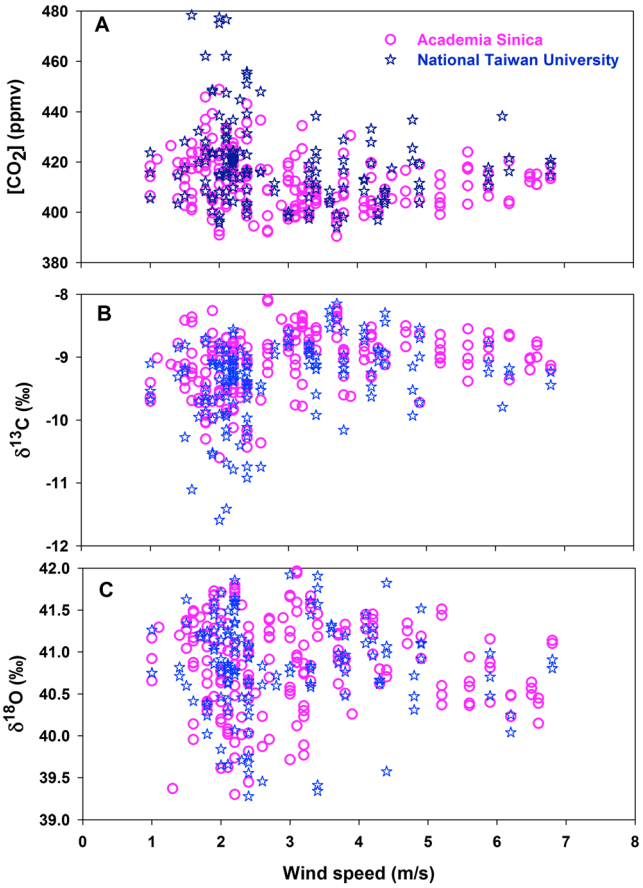

Figure 10. Changes in mixing ratio and isotopic compositions due to change in wind speed.

in downtown Taipei. Second, the site is influenced by C_4 plant respiration and yet no observable C_4 signals are seen (Figure 8).

Figure 9 shows the Keeling plot for $\delta^{18}O$ at AS and NTU. The correlation is weaker compared to $\delta^{13}C$. This is because $\delta^{18}O$ in CO_2 is influenced by multiple factors including liquid water in leaf and soil (Friedli et al., 1987; Gemery et al., 1996). The intercept in the present case is ~31 ‰, higher than the $\delta^{18}O$ value of the combustion CO_2 (~25 ‰) as shown in Figure 7. The higher value of the intercept in Figure 9 conforms the value reported earlier from a greenhouse experiment (Laskar & Liang, 2016). In their Figure 2e, Laskar and Liang (2016) showed that the natural cycle of CO_2 yielded an intercept of 30.68 ± 0.73 ‰, essentially the same as that in Figure 9, suggesting that the CO_2 in the region is largely affected by natural processes and that the anthropogenic alteration is not significant. The insignificance of anthropogenic emission was also demonstrated by Laskar et al. (2016a).

3.4. Influence From Long-Range Transported CO_2

Long-range transport of pollutants influences Taiwan significantly. In particular, in winter and spring seasons, pollutants originating from China and southeast Asian countries reach the region, affecting local air quality (Chao et al., 1996; D'Asaro et al., 2014; Fu et al., 1983; Qin et al., 2016; Thompson et al., 2001). The signals of long-range transport are clearly seen in remote stations such as LLN and Dongsa Island (Ou-Yang et al., 2015) and from satellite images (Figure 4). Pollutants carried by prevailing winds that brought polluted air masses in the eastern China in winter and southeast Asian regions in spring have also been reported by many researchers (e.g., Chuang et al., 2016 and references therein). We expect an increase of background CO_2 level by a few ppmv over Taipei due to long-range transported CO_2 from eastern China particularly in winter, but it is masked by highly elevated local anthropogenic emissions. In summer, influences from the surrounding oceans dominate. The regional influence is clearly shown in Figure 5 (see also Section 3.1 for a detailed description).

Another support for the presence and significance of long-range transported CO_2 in Taiwan comes from the correlation plot of CO_2 isotopocules versus wind speed. Wind speed data are taken from the meteorology station Keelung, located near the northern coast of Taiwan (Figure 1). Winter time (October–March), in particular, clearly shows that at wind speed greater than ~4 m s^{-1}, the levels of CO_2 isotopocules in Taipei converge to 408.7 ± 4.9 ppmv, −8.9 ± 0.1 ‰, and 40.8 ± 0.3 ‰ for $[CO_2]$, $\delta^{13}C$, and $\delta^{18}O$ at IES, respectively, and 415.3 ± 12.4 ppmv, −9.3 ± 0.4 ‰, and 41.0 ± 0.2 ‰ at NTU (Figure 10). The mixing ratios are higher than the background value of 399.8 ppmv. Similarly the isotopic compositions are lower than the background values of −8.5 ‰ and 41.9 ‰; the background values are taken to be the averaged values observed at MLO during the measurement period. This indicates that the local background CO_2 concentration and isotopic values in Taipei are set regionally, influenced by transported CO_2 when wind speed is high.

In short, it is obvious that the long-range transport plays a crucial role and needs proper assessment for precisely estimating local CO_2 emissions, which in turn provide an important constraint on anthropogenic emission from atmospheric CO_2 measurements (the top down approach). With more constraints on the transported CO_2, the influence of anthropogenic alteration on biological emissions can be better studied. More systematic studies including measurements both in day and night time with a better spatial coverage, in addition to the more sophisticated clumped and triple oxygen isotopes analyses, are underway.

4. Conclusions

CO_2 retrieved from OCO-2 satellite and CarbonTracker and wind data from ECMWF indicate that the CO_2 over Taiwan is influenced by long-range transported CO_2 from northern continents during winter and

southeast Asian countries during spring. An elevation of CO_2 mixing ratio by ~2 ppmv was observed in a remote high mountain station in spring, which is due to combined contribution of fossil fuel combustion and biomass burning in China and the Indochina peninsular region. In urban and sub-urban areas, the CO_2 mixing ratios are higher than the background mainly due to local anthropogenic emissions. Part of the seasonal variation in the background CO_2 and its isotopic composition is attributed to the long-range transported CO_2 from China and southeast Asia, specifically in winter and spring but could not be resolved with the present measurements. Contribution of anthropogenic CO_2 is estimated to be 3.0 to 5.5% and 2.0 to 5.0% at urban and sub-urban stations, respectively. Sophisticated EEMD analysis, successfully reveals the seasonal variations in the reported all three CO_2 isotopocules and also shows that the semi-annual cycle amplitude is comparable to the annual cycle amplitude. The phase correlation between the retrieved $\delta^{13}C$ and [CO_2] seasonal cycles verifies the integrity of the method in deriving the oscillations. More systematic studies combining mixing ratios and multiple isotopic compositions over the region covering more urban and remote areas over ocean may help precisely constrain the contribution of CO_2 transported from the Asian continents. Incorporation of more tracers such as clumped and triple oxygen isotopes in atmospheric CO_2 will help better identify the regional sources of CO_2, their emission rates, and transport, which are being undertaken in the region.

Acknowledgments
We thank Hao-Wei Wei, Kuei-Pin Chang, and Chia-Li Chen for collecting air samples and Wei-Kang Ho for laboratory setups. This work is supported by the Ministry of Science and Technology (MOST-Taiwan) grants 105-2111-M-001-006-MY3 to Academia Sinica. XJ is supported by NASA grants NNX13AC04G and NNX13AK34G. We thank NOAA and JMA for making the CO_2 data available for the study and WMO World Data Centre for Greenhouse Gases for providing the data through website http://ds.data.jma.go.jp/gmd/wdcgg/cgi-bin/wdcgg/catalogue.cgi. We also thank the NOAA/ARL for providing the HYSPLIT trajectory model data through website (http://ready.arl.noaa.gov). We thank the two reviewers for their suggestions that improved the Manuscript. All the data used in the manuscript are also presented in Supplementary Information.

References

Akimoto, H. (2003). Global air quality and pollution. *Science*, *302*(5651), 1716–1719. https://doi.org/10.1126/science.1092666

Ambrose, J. L., Reidmiller, D. R., & Jaffe, D. A. (2011). Causes of high O3 in the lower free troposphere over the pacific northwest as observed at the Mt. Bachelor observatory. *Atmospheric Environment*, *45*(30), 5302–5315. https://doi.org/10.1016/j.atmosenv.2011.06.056

Andres, R. J., Marland, G., Boden, T. A., & Bischof, S. (2000). Carbon dioxide emissions from fossil fuels consumption and cement manufacture, 1751–1991, and an estimate of their isotopic composition and latitudinal distribution. In T. M. L. Wigley & D. S. Schimel (Eds.), *The Carbon Cycle* (pp. 53–62). New York: Cambridge University Press. https://doi.org/10.1017/CBO9780511573095.005

Ashfold, M. J., Pyle, J. A., Robinson, A. D., Meneguz, E., Nadzir, M. S. M., Phang, S. M., et al. (2015). Rapid transport of east Asian pollution to the deep tropics. *Atmospheric Chemistry and Physics*, *15*(6), 3565–3573. https://doi.org/10.5194/acp-15-3565-2015

Benninkmeijer, C. A. M., Kraft, P., & Mook, W. G. (1983). Oxygen isotope fractionation between CO_2 and H_2O. *Chemical Geology*, *41*, 181–190. https://doi.org/10.1016/S0009-2541(83)80015-1

Bey, I., Jacob, D. J., Logan, J. A., & Yantosca, R. M. (2001). Asian chemical outflow to the Pacific in spring: Origins, pathways, and budgets. *Journal of Geophysical Research*, *106*(D19), 23,097–23,113. https://doi.org/10.1029/2001JD000806

Bush, S. E., Pataki, D. E., & Ehleringer, J. R. (2007). Sources of variation in delta C-13 of fossil fuel emissions in Salt Lake City, USA. *Applied Geochemistry*, *22*(4), 715–723. https://doi.org/10.1016/j.apgeochem.2006.11.001

Chang, C. P., Wang, Z., McBride, J., & Liu, C. H. (2005). Annual cycle of Southeast Asia—Maritime continent rainfall and the asymmetric monsoon transition. *Journal of Climate*, *18*(2), 287–301. https://doi.org/10.1175/JCLI-3257.1

Chao, S. Y., Shaw, P. T., & Wu, S. Y. (1996). El Nino modulation of the South China Sea circulation Prog. *Oceanography*, *38*, 51–93.

Chen, Y., & Ma, J. (2014). Random noise attenuation by f-x empirical-mode decomposition predictive filtering. *Geophysics*, *79*(3), V81–V91. https://doi.org/10.1190/geo2013-0080.1

Chi, K. H., Hung, N. T., Lin, C. Y., Wang, S. H., Ou-Yang, C. F., Lee, C. T., & Lin, N. H. (2016). Evaluation of atmospheric PCDD/fs at two high-altitude stations in Vietnam and Taiwan during Southeast Asia biomass burning. *Aerosol and Air Quality Research*, *16*(11), 2706–2715. https://doi.org/10.4209/aaqr.2015.11.0653

Chuang, M. T., Lee, C. T., Chou, C. C. K., Engling, G., Chang, S. Y., Chang, S. C., et al. (2016). Aerosol transport from Chiang Mai, Thailand to Mt. Lulin, Taiwan implication of aerosol aging during long-range transport. *Atmospheric Environment*, *137*, 101–112.

Ciais, P., Tans, P. P., Trolier, M., White, J. W. C., & Francey, R. J. (1995). A large northern hemispheric terrestrial CO_2 sink indicated by the $^{13}C/^{12}C$ ratio of atmospheric CO_2. *Science*, *269*(5227), 1098–1102. https://doi.org/10.1126/science.269.5227.1098

Clark-Thorne, S. T., & Yapp, C. J. (2003). Stable isotope constraints on mixing and mass balance of CO2 in an urban atmosphere: Dallas metropolitan area, TX, USA. *Applied Geochemistry*, *18*(1), 75–95. https://doi.org/10.1016/S0883-2927(02)00054-9

Cooper, O. R., Parrish, D. D., Stohl, A., Trainer, M., Nédélec, P., Thouret, V., et al. (2010). Increasing springtime ozone mixing ratios in the free troposphere over western North America. *Nature*, *463*(7279), 344–348. https://doi.org/10.1038/nature08708

Coutts, A. M., Beringer, J., & Tapper, N. J. (2007). Characteristics influencing the variability of urban CO2 fluxes in Melbourne, Australia. *Atmospheric Environment*, *41*(1), 51–62. https://doi.org/10.1016/j.atmosenv.2006.08.030

Crisp, D., Atlas, R. M., Breon, F. M., Brown, L. R., Burrows, J. P., Ciais, P., et al. (2004). The orbiting carbon observatory (OCO) mission. *Advances in Space Research*, *34*(4), 700–709. https://doi.org/10.1016/j.asr.2003.08.062

Crisp, D., Pollock, H. R., Rosenberg, R., Chapsky, L., Lee, R. A. M., Oyafuso, F. A., et al. (2016). The on-orbit performance of the orbiting carbon Observatory-2 (OCO-2) instrument and its radiometrically calibrated products. *Atmospheric Measurement Techniques Discussions*, 1–45. https://doi.org/10.5194/amt-2016-281

Crutzen, P. J., & Andreae, M. O. (1990). Biomass burning in the tropics: Impact on atmospheric chemistry and biogeochemical cycles. *Science*, *250*(4988), 1669–1678.

D'Asaro, E. A., Black, P. G., Centurioni, L. R., Chang, Y.-T., Chen, S. S., Foster, R. C., et al. (2014). Impact of typhoons on the ocean in the pacific. *American Meteorological Society*, *95*(9), 1405–1418. https://doi.org/10.1175/BAMS-D-12-00104.1

Dee, D. P., Uppala, S. M., Simmons, A. J., Berrisford, P., Poli, P., Kobayashi, S., et al. (2011). The ERA-interim reanalysis: Configuration and performance of the data assimilation system. *Quarterly Journal of the Royal Meteorological Society*, *137*(656), 553–597. https://doi.org/10.1002/qj.828

Deines, P. (1980). The isotopic composition of reduced organic carbon. In P. Fritz & J. C. Fontes (Eds.), *Handbook of Environmental Isotope Geochemistry, 1. The Terrestrial Environment* (pp. 329–406). New York: Elsevier.

Demeny, A., & Haszpra, L. (2002). Stable isotope compositions of CO_2 in background air and at polluted sites in Hungary. *Rapid Communications in Mass Spectrometry*, *16*(8), 797–804. https://doi.org/10.1002/rcm.640

Draxler, R. R., & Rolph, G. D. (2014). HYSPLIT (HYbrid Single-Particle Lagrangian Integrated Trajectory) Model access via NOAA ARL READY (http://ready.arl.noaa.gov/HYSPLIT.php)

Duren, R. M., & Miller, C. E. (2012). Measuring the carbon emissions of megacities. *Nature Climate Change*, *2*(8), 560–562. https://doi.org/10.1038/nclimate1629

Francey, R. J., Gifford, R. M., Sharkey, T. D., & Weir, B. (1985). Physiological influences on carbon isotope discrimination in huon pine (Lagarostrobos franklinii). *Oecologia*, *66*(2), 211–218. https://doi.org/10.1007/BF00379857

Friedli, H., Siegenthaler, U., Rauber, D., & Oeschger, H. (1987). Measurements of concentration, $^{13}C/^{12}C$ and $^{18}O/^{16}O$ ratios of tropospheric carbon dioxide over Switzerland. *Tellus*, *39B*(1-2), 80–88. https://doi.org/10.1111/j.1600-0889.1987.tb00272.x

Fu, C., Fletcher, J., & Slutz, R. (1983). The structure of the Asian monsoon surface wind field over the ocean. *Journal of Climate and Applied Meteorology*, *22*(7), 1242–1252. https://doi.org/10.1175/1520-0450(1983)022<1242:TSOTAM>2.0.CO;2

Fung, I., Field, C. B., Berry, J. A., Thompson, M. V., Randesron, J. T., Malmström, C. M., et al. (1997). Carbon 13 exchanges between the atmosphere and biosphere. *Global Biogeochemical Cycles*, *11*(4), 507–533.

Gemery, P. A., Trolier, M., & White, J. W. C. (1996). Oxygen isotope exchange between carbon dioxide and water following atmospheric sampling using glass flasks. *Journal of Geophysical Research*, *101*(D9), 14,415–14,420. https://doi.org/10.1029/96JD00053

Guha, T., & Ghosh, P. (2014). Diurnal and seasonal variation of mixing ratio and $\delta^{13}C$ of air CO_2 observed at an urban station Bangalore, India. *Environmental Science and Pollution Research International*, *22*(3), 1877–1890. https://doi.org/10.1007/s11356-014-3530-3

Hoell, J. M., Davis, D. D., Liu, S. C., Newell, R. E., Akimoto, H., McNeal, R. J., & Bendura, R. J. (1997). The pacific exploratory mission-west phase B: February-march, 1994. *Journal of Geophysical Research*, *102*(D23), 28,223–28,239. https://doi.org/10.1029/97JD02581

International Energy Agency (2008). *World Energy Outlook, 2008 Rep*. Paris, France: IEA. https://doi.org/10.1787/weo-2008-en

International Energy Agency (2017). *CO_2 emission from fossil fuel combustion Highlights* (2017th ed.). Paris: OECD/IEA.

Jacob, D. J., Crawford, J. H., Kleb, M. M., Connors, V. S., Bendura, R. J., Raper, J. L., et al. (2003). Transport and chemical evolution over the pacific (TRACE-P) aircraft mission: Design, execution, and first results. *Journal of Geophysical Research*, *108*(D20), 9000. https://doi.org/10.1029/2002JD003276

Jaffe, D., McKendry, I., Anderson, T., & Price, H. (2003). Six 'new' episodes of trans-pacific transport of air pollutants. *Atmospheric Environment*, *37*(3), 391–404. https://doi.org/10.1016/S1352-2310(02)00862-2

Jiang, X., Chahine, M. T., Li, Q., Liang, M. C., Olsen, E. T., Chen, L. L., et al. (2012). CO_2 semiannual oscillation in the middle troposphere and at the surface, global Biogeochem. *Cycle*, *26*, GB3006. https://doi.org/10.1029/2011GB004118

Jiang, X., Crisp, D., Olsen, E. T., Kulawik, S. S., Miller, C. E., Pagano, T. S., et al. (2016). CO_2 annual and semiannual cycles from multiple satellite retrievals and models. *Earth and Space Sciences*, *3*(2), 78–87. https://doi.org/10.1002/2014EA000045

Jurikova, H., Guha, T., Abe, O., Shiah, F. K., Wang, C. H., & Liang, M. C. (2016). Variations in triple isotope composition of dissolved oxygen and primary production in a subtropical reservoir. *Biogeosciences*, *13*(24), 6683–6698. https://doi.org/10.5194/bg-13-6683-2016

Keeling, C. D., Bacastrow, R. B., Carter, A. F., Piper, S. C., Whorf, T. P., Heimann, M., et al. (1989). A three-dimensional model of atmospheric CO_2 transport based on observed winds: 1. Analysis of observational data. In *Aspects of Climate Variability in the Pacific and the Western Americas*, *Geophysical Monograph Series* (Vol. 55, pp. 165–236). Washington, DC: American Geophysical Union.

Keeling, C. D., Mook, W. G., & Tans, P. P. (1979). Recent trends in the $^{13}C/^{12}C$ ratio of atmospheric carbon dioxide. *Nature*, *277*(5692), 121–123. https://doi.org/10.1038/277121a0

Keeling, C. D., Whorf, T. P., Wahlen, M., & van der Plicht, J. (1995). Interannual extremes in the rate and rise of atmospheric carbon dioxide since 1980. *Nature*, *375*(6533), 666–670. https://doi.org/10.1038/375666a0

Kondo, Y., Ko, M., Koike, M., Kawakami, S., & Ogawa, T. (2002). Preface to special section on biomass burning and lightning experiment (BIBLE). *Journal of Geophysical Research*, *108*(D3), 8397. https://doi.org/10.1029/2002JD002401

Kort, E. A., Frankenberg, C., Miller, C. E., & Oda, T. (2012). Space-based observations of megacity carbon dioxide. *Geophysical Research Letters*, *39*, L17806. https://doi.org/10.1029/2012GL052738

Kuang, Z. M., Margolis, J., Toon, G., Crisp, D., & Yung, Y. L. (2002). Spaceborne measurements of atmospheric CO_2 by high-resolution NIR spectrometry of reflected sunlight: An introductory study. *Geophysical Research Letters*, *29*(15), 1716. https://doi.org/10.1029/2001GL014298

Kuc, T. (1986). Carbon isotopes in atmospheric CO_2 of the Krakow region: A two-year record. *Radiocarbon*, *28*(2A), 649–654. https://doi.org/10.1017/S0033822200007840

Kuc, T. (1991). Concentration and carbon isotopic composition of atmospheric CO_2 in southern Poland. *Tellus Series B*, *43*, 373–378.

Kuc, T., Rozanski, K., Zimnoch, M., Necki, J., Chmura, L., & Jelen, D. (2007). Two decades of regular observations of (CO2)-C-14 and (CO2)-C-13 content in atmospheric carbon dioxide in Central Europe: Long-term changes of regional anthropogenic fossil CO_2 emissions. *Radiocarbon*, *49*(02), 807–816. https://doi.org/10.1017/S0033822200042685

Kuc, T., & Zimnoch, M. (1998). Changes of the CO2 sources and sinks in a polluted urban area (southern Poland) over the last decade, derived from the carbon isotope composition. *Radiocarbon*, *40*(1), 417–423.

Kuze, A., Suto, H., Nakajima, M., & Hamazaki, T. (2009). Thermal and near infrared sensor for carbon observation Fourier transform spectrometer on the greenhouse gases observing satellite for greenhouse gases monitoring. *Applied Optics*, *48*(35), 6716–6733. https://doi.org/10.1364/AO.48.006716

Laskar, A. H., Huang, J. C., Hsu, S. C., Bhattacharya, S. K., Wang, C. H., & Liang, M. C. (2014). Stable isotopic composition of near surface atmospheric water vapor and rain–vapor interaction in Taipei, Taiwan. *Journal of Hydrology*, *519*, 2091–2100. https://doi.org/10.1016/j.jhydrol.2014.10.017

Laskar, A. H., & Liang, M. C. (2016). Clumped isotopes in near surface atmospheric CO_2 over land, coast and ocean in Taiwan and its vicinity. *Biogeosciences*, *13*, 1–44. https://doi.org/10.5194/bg-2016-106

Laskar, A. H., Mahata, S., & Liang, M. C. (2016b). Identification of anthropogenic CO_2 using triple oxygen and clumped isotpes. Environmental science and technology. *Environmental Science & Technology*, *50*(21), 11,806–11,814. https://doi.org/10.1021/acs.est.6b02989

Laskar, A. H., Yadava, M. G., & Ramesh, R. (2016a). Stable and radioactive carbon in forest soils of Chhattisgarh, Central India: Implications for tropical soil carbon dynamics and stable carbon isotope evolution. *Journal of Asian Earth Sciences*, *123*, 47–57. https://doi.org/10.1016/j.jseaes.2016.03.021

Laskar, A. H., Yadava, M. G., Sharma, N., & Ramesh, R. (2013). Late Holocene climate in the lower Narmada valley, Gujarat, Western India, inferred using sedimentary carbon and oxygen isotope ratios. *The Holocene*, *23*(8), 1115–1122.

Laskar, A. H., Yui, T. F., & Liang, M. C. (2016c). Clumped isotope composition of marbles from the backbone range of Taiwan. *Terra Nova*, *28*(4), 265–270. https://doi.org/10.1111/ter.12217

Liang, M. C., & Mahata, S. (2015). Oxygen anomaly in near surface carbon dioxide reveals deep stratospheric intrusion. *Scientific Reports*, *5*(11352), 2015.

Liang, M. C., Mahata, S., Laskar, A. H., & Bhattacharya, S. K. (2016). Spatiotemporal variability of oxygen isotope anomaly in near surface air CO_2 over urban, Semi-Urban and Ocean Areas in and around Taiwan. *Aerosol and Air Quality Research*, *17*(3), 706–720. https://doi.org/10.4209/aaqr.2016.04.0171

Liang, M. C., Mahata, S., Laskar, A. H., Thiemens, M. H., & Newman, S. (2018). Oxygen Isotope Anomaly in Tropospheric CO2 and Implications for CO2 Residence Time in the Atmosphere and Gross Primary Productivity. *Scientific Reports*, *7*(1), 13180. https://doi.org/10.1038/s41598-017-12774-w

Liang, Q., Jaegle, L., Jaffe, D. A., Weiss-Penzias, P., Heckman, A., & Snow, J. A. (2004). Long-range transport of Asian pollution to the northeast pacific: seasonal variations and transport pathways of carbon monoxide. *Journal of Geophysical Research*, *109*, D23S07. https://doi.org/10.1289/ehp.11463

Lin, N. H., Sayer, A. M., Wang, S. H., Loftus, A. M., Hsiao, T. C., Sheu, G. R., et al. (2014). Interactions between biomass-burning aerosols and clouds over Southeast Asia: Current status, challenges, and perspectives. *Environmental Pollution*, *195*, 292–307. https://doi.org/10.1016/j.envpol.2014.06.036

Lin, N. H., Tsay, S. C., Maring, H. B., Yen, M. C., Sheu, G. R., Wang, S. H., et al. (2013). An overview of regional experiments on biomass burning aerosols and related pollutants in Southeast Asia: From BASE-ASIA and the Dongsha experiment to 7-SEAS. *Atmospheric Environment*, *78*, 1–19. https://doi.org/10.1016/j.atmosenv.2013.04.066

Liu, H. Y., Jacob, D. J., Bey, I., Yantosca, R. M., Duncan, B. N., & Sachse, G. W. (2003). Transport pathways for Asian pollution outflow over the pacific: Interannual and seasonal variations. *Journal of Geophysical Research*, *108*(D20), 8786. https://doi.org/10.1029/2002JD003102

Liu, Z., Yang, H., & Liu, Q. (2001). Regional dynamics of seasonal variability in the South China Sea J. *Physical Oceanography*, *31*(1), 272–284. https://doi.org/10.1175/1520-0485(2001)031<0272:RDOSVI>2.0.CO;2

Luz, B., & Barkan, E. (2011). The isotopic composition of atmospheric oxygen. *Global Biogeochemical Cycles*, *25*, GB3001. https://doi.org/10.1029/2010GB003883

Mahata, S., Bhattacharya, S. K., Wang, C. H., & Liang, M. C. (2012). An improved CeO_2 method for high precision measurements of $^{17}O/^{16}O$ ratios for atmospheric carbon dioxide. *Rapid Communications in Mass Spectrometry*, *26*(17), 1909–1922. https://doi.org/10.1002/rcm.6296

Mehta, N., Dinakaran, J., Patel, S., Laskar, A. H., Yadava, M. G., Ramesh, R., & Krishnayya, N. R. S. (2013). Changes in litter decomposition and soil organic carbon in a reforested tropical deciduous cover (India). *Ecological Research*, *28*, 239–248.

Metzger, E. J. (2003). Upper Ocean sensitivity to wind forcing in the South China Sea. *Journal of Oceanography*, *59*(6), 783–798. https://doi.org/10.1023/B:JOCE.0000009570.41358.c5

Miller, C. E., Crisp, D., DeCola, P. L., Olsen, S. C., Randerson, J. T., Michalak, A. M., et al. (2007). Precision requirements for space-based X-CO_2 data. *Journal of Geophysical Research*, *112*, D10314. https://doi.org/10.1029/2006JD007659

Miller, J. B., & Tans, P. P. (2003). Calculating isotopic fractionation from atmospheric measurements at various scales. *Tellus*, *55*(2), 207–214. https://doi.org/10.1034/j.1600-0889.2003.00020.x

Mook, W. G., Koopmans, M., Carter, A. F., & Keeling, C. D. (1983). Seasonal, latitudinal, and secular variations in the abundance and isotopic ratios of atmospheric carbon dioxide: 1. Results from land stations. *Journal of Geophysical Research*, *88*(C15), 10,915–10,933. https://doi.org/10.1029/JC088iC15p10915

Nakajima, T., Yoon, S. C., Ramanathan, V., et al. (2007). Over view of the atmospheric brown cloud east asian regional experiment 2005 and a study of the aerosol direct radiative forcing in east Asia. *Journal of Geophysical Research*, *112*, D24S91. https://doi.org/10.1029/2007JD009009

Newman, S., Xu, X., Affek, H. P., Stolper, E., & Epstein, S. (2008). Changes in mixing ratio and isotopic composition of CO_2 in urban air from the Los Angeles basin, California, between 1972 and 2003. *Journal of Geophysical Research*, *113*, D23304. https://doi.org/10.1029/2008JD009999

Nguyen, B. C., Mihalopoulos, N., & Putaud, J. P. (1994). Rice straw burning in Southeast Asia as a source of CO and COS to the atmosphere. *Journal of Geophysical Research*, *99*(D8), 16,435–16,439. https://doi.org/10.1029/93JD03521

Nieuwolt, S. (1977). *Tropical Climatology: An Introduction to the Climates of Low Latitudes*. New York: John Wiley.

Ohara, T., Akimoto, H., Kurokawa, J., Horii, N., Yamaji, K., Yan, X., & Hayasaka, T. (2007). An Asian emission inventory of anthropogenic emission sources for the period 1980-2020. *Atmospheric Chemistry and Physics*, *7*(16), 4419–4444. https://doi.org/10.5194/acp-7-4419-2007

Ou-Yang, C. F., Lin, N. H., Lin, C. C., Wang, S. H., Sheu, G. R., Lee, C. T., et al. (2014). Characteristics of atmospheric carbon monoxide at a high mountain background station in East Asia. *Atmospheric Environment*, *89*, 613–622. https://doi.org/10.1016/j.atmosenv.2014.02.060

Ou-Yang, C. F., Lin, N. H., Sheu, G. R., Lee, C. T., & Wang, J. L. (2012). Seasonal and diurnal variations of ozone at a high-altitude mountain baseline station in East Asia. *Atmospheric Environment*, *46*, 279–288. https://doi.org/10.1016/j.atmosenv.2011.09.060

Ou-Yang, C. F., Yen, M. C., Lin, T. H., Wang, J. L., Schnell, R. C., Lang, P. M., et al. (2015). Impact of equatorial and continental airflow on primary greenhouse gases in the northern South China Sea. *Environmental Research Letters*, *10*(6), 065005. https://doi.org/10.1088/1748-9326/10/6/065005

Pataki, D., Bowling, D. R., Ehleringer, J. R., & Zobitz, J. M. (2006). High resolution atmospheric monitoring of carbon dioxide sources. *Geophysical Research Letters*, *33*, L03813. https://doi.org/10.1029/2005GL024822

Pataki, D. E., Bowling, D. R., & Ehleringer, J. R. (2003). Seasonal cycle of carbon dioxide and its isotopic composition in an urban atmosphere: anthropogenic and biogenic effects. *Journal of Geophysical Research*, *108*(D23), 4735. https://doi.org/10.1029/2003JD003865

Pataki, D. E., Ehleringer, J. R., Flanagan, L. B., Yakir, D., Bowling, D. R., Still, C. J., et al. (2003). The application and interpretation of keeling plots in terrestrial carbon cycle research. *Global Biogeochemical Cycles*, *17*(1), 1022. https://doi.org/10.1029/2001GB001850

Pataki, D. E., Xu, T., Luo, Y. Q., & Ehleringer, J. R. (2007). Inferring biogenic and anthropogenic carbon dioxide sources across an urban to rural gradient. *Oecologia*, *152*(2), 307–322. https://doi.org/10.1007/s00442-006-0656-0

Peters, W., Jacobson, A. R., Sweeney, C., Andrews, A. E., Conway, T. J., Masarie, K., et al. (2007). An atmospheric perspective on north American carbon dioxide exchange: CarbonTracker. *Proceedings of the National Academy of Sciences of the United States of America*, *104*(48), 18,925–18,930. https://doi.org/10.1073/pnas.0708986104

Pochanart, P., Akimoto, H., Kajii, Y., Potemkin, V. M., & Khodzher, T. V. (2003). Regional background ozone and carbon monoxide variations in remote Siberia/East Asia. *Journal of Geophysical Research*, *108*(D1), 4028. https://doi.org/10.1029/2001JD001412

Pochanart, P., Wild, O., & Akimoto, H. (2004). Air pollution import to and export from East Asia. In A. Stohl (Ed.), *Hand Book of Environmental Chemistry* (pp. 99–130). Berlin: Springer.

Qin, X., Wang, F., Deng, C., Wang, F., & Yu, G. (2016). Seasonal variation of atmospheric particulate mercury over the East China Sea, an outflow region of anthropogenic pollutants to the open Pacific Ocean. *Atmospheric Pollution Research*, *7*(5), 876–883. https://doi.org/10.1016/j.apr.2016.05.004

Rangarajan, R., Laskar, A. H., Bhattacharya, S. K., Shen, C. C., & Liang, M. C. (2017). An insight into the western Pacific wintertime moisture sources using dual water vapor isotopes. *Journal of Hydrology*, *547*, 111–123. https://doi.org/10.1016/j.jhydrol.2017.01.047

Reid, J., Hyer, E., Johnson, R., Holben, B. N., Yokelson, R., Zhang, J., et al. (2013). Observing and understanding the southeast Asian aerosol system by remote sensing: An initial review and analysis for the seven southeast Asian studies (7SEAS) program. *Atmospheric Research*, *122*, 403–468. https://doi.org/10.1016/j.atmosres.2012.06.005

Sirignano, C., Neubert, R. E. M., & Meijer, H. A. J. (2004). N_2O influence on isotopic measurements of atmospheric CO_2. *Rapid Communications in Mass Spectrometry*, *18*(16), 1839–1846. https://doi.org/10.1002/rcm.1559

Tans, P. P. (1981). $^{13}C/^{12}C$ of industrial CO_2. In B. Bolin (Ed.), *Carbon Cycle Modelling* (pp. 127–129). Chichester, UK: John Wiley.

Tans, P. P., Fung, I. Y., & Takahashi, T. (1990). Observational contraints on the global atmospheric CO_2 budget. *Science*, *247*(4949), 1431–1439.

Thirumalai, K., DiNezio, P. N., Okumura, Y., & Deser, K. (2017). Extreme temperatures in Southeast Asia caused by El Niño and worsened by global warming. *Nature Communications*, *8*, 15,531. https://doi.org/10.1038/ncomms15531

Thompson, A. M., Witte, J. C., Hudson, R. D., Guo, H., Herman, J. R., & Fujiwara, M. (2001). Tropical tropospheric ozone and biomass burning. *Science*, *291*(5511), 2128–2132. https://doi.org/10.1126/science.291.5511.2128

Tsay, S. C., Hsu, N. C., Lau, W. K. M., Li, C., Gabriel, P. M., Ji, Q., et al. (2013). From BASE-ASIA toward 7-SEAS: A satellitesurface perspective of boreal spring biomass-burning aerosols and clouds in Southeast Asia. *Atmospheric Environment*, *78*, 20–34. https://doi.org/10.1016/j.atmosenv.2012.12.013

Vadrevu, K. P., Ellicott, E., Giglio, L., Badarinath, K. V. S., Vermote, E., Justice, C., & Lau, W. K. M. (2012). Vegetation fires in the himalayan region - aerosol load, black carbon emissions and smoke plume heights. *Atmospheric Environment*, *47*, 241–251. https://doi.org/10.1016/j.atmosenv.2011.11.009

Wai, K. M., & Tanner, P. A. (2014). Recent springtime regionalCO variability in southern China and the adjacent ocean: Anthropogenic and biomass burning contribution. *Aerosol and Air Quality Research*, *14*(1), 21–32. https://doi.org/10.4209/aaqr.2013.05.0159

Wang, T., Ding, A. J., Blake, D. R., Zahorowski, W., Poon, C. N., & Li, Y. S. (2003). Chemical characterization of the boundary layer outflow of air pollution to Hong Kong during February-April 2001. *Journal of Geophysical Research*, *108*(D20), 8787. https://doi.org/10.1029/2002JD003272

Widory, D., & Javoy, M. (2003). The carbon isotope composition of atmospheric CO_2 in Paris. *Earth and Planetary Science Letters*, *215*(1–2), 289–298. https://doi.org/10.1016/S0012-821X(03)00397-2

Wild, O., & Akimoto, H. (2001). Intercontinental transport of ozone and its precursors in a three-dimensional global CTM. *Journal of Geophysical Research*, *106*(D21), 27,729–27,744. https://doi.org/10.1029/2000JD000123

Worden, J., Doran, G., Kulawik, S., Eldering, A., Crisp, D., Frankenberg, C., et al. (2016). Evaluation and attribution of OCO-2 XCO2 uncertainties. *Atmospheric Measurement Techniques Discussions*, 1–28. https://doi.org/10.5194/amt-2016-175

World Bank (2010). *Cities and Climate Change: An Urgent Agenda*. Washington, DC: Rep., World Bank.

Wu, Z., & Huang, N. E. (2009). Ensemble empirical mode decomposition: A noise-assisted data analysis method. *Adv. Adapt. Data Anal.*, *01*(03), 339–372. https://doi.org/10.1142/S1793536909000187

Wunch, D., Wennberg, P. O., Osterman, G., Fisher, B., Naylor, B., Roehl, C. M., et al. (2016). Comparisons of the orbiting carbon Observatory-2 (OCO-2) XCO2 measurements with TCCON. *Atmospheric Measurement Techniques Discussions*, 1–45. https://doi.org/10.5194/amt-2016-227

Yokota, T., Yoshida, Y., Eguchi, N., Ota, Y., Tanaka, T., Watanabe, H., & Maksyutov, S. (2009). Global concentrations of CO_2 and CH_4 retrieved from GOSAT: First preliminary results. *Solaiat*, *5*, 160–163. https://doi.org/10.2151/sola.2009-041

Zhang, Y., Sperber, K. R., & Boyle, J. S. (1997). Climatology and interannual variation of the east Asian winter monsoon: Results from the 1979-95 NCEP/NCARreanalysis. *Monthly Weather Review*, *125*(10), 2605–2619. https://doi.org/10.1175/1520-0493(1997)125<2605:CAIVOT>2.0.CO;2